BIOCELL
2021 45(4): 901-910

Tech Science Press

Circular RNA circFOXM1 triggers the tumorigenesis of non-small cell lung cancer through miR-132-3p/TMEM14A axis

Weigao ZHONG[1,*]; Aiqin CHEN[2]; Xiaohong TANG[1]; Yi LIU[1]

[1] Department of Respiratory, Sichuan Mianyang 404 Hospital, Mianyang, 621000, China
[2] Department of Electrocardiogram Room, Wuxi Puren Medical Group, Wuxi, 214000, China

Key words: circFOXM1, miR-132-3p, TMEM14A, Non-small cell lung cancer, Proliferation

Abstract: Earlier studies indicated that circular RNAs (circRNAs) were found in various cancer cells, and circFOXM1 was reported to act as an oncogene in non-small cell lung cancer (NSCLC). However, the function of circFOXM1 in NSCLC remains unclear. The expression levels of genes were measured using quantitative real-time polymerase chain reactions (qRT-PCR). Cell proliferation and apoptosis were determined by 3-(4,5-dimethylthiazol-2-yl)-2,5-diphenyltetrazolium bromide solution (MTT) and flow cytometry assay. The relative protein expression was assessed by western blot. Moreover, transwell assays were employed to examine cell migration and invasion. The targeted relationship was confirmed by dual-luciferase reporter assay. The expression of circFOXM1 was up-regulated in NSCLC tissues and cell lines. The depletion of circFOXM1 decreased the proliferation, migration, invasion, and induced cell apoptosis of NSCLC cells. MicroRNA-132-3p (MiR-132-3p) was identified as a target of circFOXM1. The expression level of miR-132-3p was decreased in NSCLC tissues and cell lines and inversely correlated with circFOXM1 expression. Furthermore, the effects of circFOXM1 down-regulation on NSCLC cell progression were abolished by miR-132-3p inhibitor. Transmembrane protein 14A (TMEM14A) was verified as a target gene of miR-132-3p. The effects of circFOXM1 depletion on NSCLC cell proliferation, apoptosis, migration, and invasion were reversed by TMEM14A overexpression. Our study demonstrated that knockdown of circFOXM1 suppressed NSCLC progression through regulating miR-132-3p/TMEM14A axis, suggesting the circFOXM1/miR-132-3p/TMEM14A axis may serve as the novel target for NSCLC diagnosis and therapy.

Introduction

Lung cancer with high incidence and mortality is a growing threat to humans in the world. It has been reported that non-small cell lung cancer (NSCLC) accounted for about 85% of lung cancer, while lung cancer caused 20% of cancer-related deaths (Jemal *et al.*, 2011; Didkowska *et al.*, 2016). In recent years, the diagnosis and treatment strategies have been improved, but the overall 5-year survival rate remains around 20% (Li *et al.*, 2019a). At present, a surgical operation is the main treatment for lung cancer, and postoperative recurrence and metastasis are important factors affecting the survival rate of lung cancer patients (Wang *et al.*, 2019c). Therefore, it is urgent to find the novel molecular mechanism to develop new therapies for NSCLC.

Circular RNA (circRNA), a newly discovered abundant RNA species, is a noncoding covalent closed RNA formed by exon and intron sequences (Liu *et al.*, 2019a). CircRNA is characterized by its evolutionary conservation and tissue-specific expression, which is more stable than linear miRNA (Jeck *et al.*, 2013; Memczak *et al.*, 2013). Many studies reported that circRNA negatively regulated miRNA expression, cell function, and tumor progression through different mechanisms (Chen *et al.*, 2015; Li and Huang, 2017; Kristensen *et al.*, 2018). CircFOXM1 is a newly discovered cancer-related cycle RNA with a length of 3410 nucleotides. CircFOXM1 was highly expressed in NSCLC tissues and cells and was associated with poor prognosis, circFOXM1 was confirmed to affect the proliferation and migration of lung cancer cells (Liu *et al.*, 2019b). However, the regulatory mechanism of circFOXM1 in NSCLC progression has been rarely reported.

MicroRNAs (miRNAs/miRs) are a group of single-stranded non-coding RNAs that are involved in post-transcriptional gene regulation by binding to the 3' untranslated region (UTR) of target RNA and regulate gene expression by regulating the post-transcriptional level of the target RNA (Macfarlane and Murphy (2010); Chen *et al.*, 2019). A previous study demonstrated that circRNAs acted as sponges of miRNAs in various cancers (Taborda *et al.*, 2017).

*Address correspondence to: Weigao Zhong, zhongweigao02@126.com
Received: 23 September 2019; Accepted: 13 May 2020

Doi: 10.32604/biocell.2021.08672

For example, circ-000926 with low expression inhibited the progression of renal cell carcinoma through nhibiting CDH2 expression by sponging miR-411 (Zhang *et al.*, 2019). In bladder cancer, circ-0023642 regulated epidermal growth factor receptor (EGFR) expression by regulating miR-490-5p expression (Wu *et al.*, 2019). Moreover, previous research reported that abnormally expressed miR-132-3p was associated with tumorigenesis (Wang *et al.*, 2019a). Other researches indicated that miR-132-3p was lowly expressed in lung cancer tissues and cells, and miR-132-3p could suppress the migration and invasion of lung cancer cells (Li *et al.*, 2015b; You *et al.*, 2014). Hence, the specific mechanism between circFOXM1 and miR-132-3p in NSCLC progression still needed further exploration.

In the study, H1299 and A549 cells were selected as the experiment material. We researched the potential biological functions of circFOXM1 in NSCLC progression *in vitro*.

Materials and Methods

Clinical samples

Thirty NSCLC tissues and their paired normal tissues were collected from NSCLC patients at Sichuan Mianyang 404 Hospital between January 2017 and May 2018. All patients signed the written informed consent, and our research was supported by the Medical Ethics Committee of Sichuan Mianyang 404 Hospital.

Cell culture

Lung normal cells 16HBE and NSCLC cell lines (SK-MES-1, H1299, A549) were acquired from the Chinese Academy of Medical Sciences (Beijing, China). 16HBE, H1299, and A549 cells were cultured in Roswell Park Memorial Institute (RPMI) 1640 (Sigma, Saint Louis, MO, USA). SK-MES-1 cells were maintained with Dulbecco's Modified Eagle's Media (DMEM, Sigma, Saint Louis, MO, USA) supplementing with 10% fetal bovine serum (FBS, Invitrogen, Carlsbad, CA, USA) and 1% penicillin-streptomycin (Solarbio, Beijing, China) at 37° with 5% CO_2.

Quantitative real-time polymerase chain reaction (qRT-PCR)

TRIzol reagent (Invitrogen, Carlsbad, CA, USA) was used to extract the total RNA. The complementary DNA (cDNA) for circFOXM1 or Transmembrane protein 14A (TMEM14A) was synthesized by PrimeScript II Kit (Takara, Kusatsu, Japan). The miRNA was transcribed into cDNA using One Step Prime Script miRNA cDNA Synthesis Kit (Takara, Kusatsu, Japan). qRT-PCR was performed using the SYBR Green Master Mix (Roche, Shanghai, China), and the data were calculated by the $2^{-\Delta\Delta CT}$ method. Glyceraldehyde-3-phosphate dehydrogenase (GAPDH) and U6 acted as internal controls. The primer sequences of GAPDH (Li *et al.*, 2019b), U6 (Li *et al.*, 2019b), circFOXM1, miR-132-3p (Wang *et al.*, 2019a) and TMEM14A (Zhang *et al.*, 2016) were shown in attachment Tab. 1.

Cell transfection

The small interfering RNA (siRNA) targeting circFOXM1 (si-circFOXM1), circFOXM1 overexpression plasmid (pcDNA-circFOXM1) and their corresponding negative control (si-NC or pcDNA-NC), miR-132-3p mimics/miR-NC, anti-miR-132-3p/anti-miR-NC and pcDNA-TMEM14A/pcDNA-NC purchased from Genepharma (Shanghai, China) were transfected into cells using Lipofectamine 3000 reagent (Invitrogen, Carlsbad, CA, USA). After 72 h, the transfection efficiency was detected using qRT-PCR.

3-(4,5-dimethylthiazol-2-yl)-2,5-diPhenyltetrazolium bromide solution (MTT) assay

MTT kit (Solarbio, Beijing, China) was applied to measure cell viability as previously recommended (Zhou *et al.*, 2016). After transfection, the cells were collected at a density of 3×10^5 cells/mL and seeded into 96-well plates. After 24 h, cells were incubated with 20 μL MTT solution at 37°C for 4 h. Then, the proliferation rates at 0, 24, 48, and 72 h were examined by a microplate reader (Thermo Scientific, Waltham, MA, USA).

Cell apoptosis assay

The apoptotic rate of H1299 and A549 cells was detected using Annexin V-fluorescein isothiocyanate (FITC)/propidium iodide (PI) apoptosis kit (Invitrogen, Carlsbad, CA, USA). Briefly, NSCCL cells (2×10^6 cells/well) were planted in the 6-well plates and incubated in medium for 48 h. Next, the

TABLE 1

The sequences of specific primers

Type	Primer name	Access number	Primer sequence (from 5' to 3')
Reference gene	GAPDH	NG_007073	Forward:5'-ATCCACGGGAGAGCGACAT-3'
			Reverse: 5'-CAGCTGCTTGTAAAGTGGAC-3'
	U6	NR_004394	Forward:5'-CAGATCTGTCGGTGTGGCAC-3'
			Reverse:5'-GGCCCCGGATTATCCGACATTC-3'
CircRNA	FOXM1	NM_202002	Forward:5'-AGCAGTCTCTTACCTTCC-3'
			Reverse: 5'-CTGGCAGTCTCTGGATAA-3'
miRNA	MiR-132-3p	MIMAT0000426	Forward:5'-GCGCGCGTAACAGTCTACAGG-3'
			Reverse:5'-GTCGTATCCAGTGCAGGGTCC-3'
Gene	TMEM14A	NM_014051	Forward:5'-GTTTGGTTGCAGGTTTAAG-3'
			Reverse:5'-AATATGCTCTGCCCATTAC-3'

transfected cells were rinsed with pre-cooling PBS and re-suspended in 100 μL binding buffer. Then, the mixture was incubated with 5 μL Annexin V-FITC and PI in the dark at 37°C for 15 min. Subsequently, the flow cytometry system (Beckman Coulter, Brea, CA, USA) was employed to analyze cell apoptosis.

Western blot assay

After transfection for 48 h, total protein was extracted from H1299 and A549 cells using RIPA buffer (Beyotime, Beijing, China), and bicinchoninic acid (BCA, Beyotime, Beijing, China) was used to assess the protein concentrations. Total protein was separated by sodium dodecyl sulfate-polyacrylamide gel electrophoresis (SDS-PAGE) and transferred to polyvinylidene difluoride (PVDF) membrane. Then, the membrane was maintained with 5% nonfat milk for 30 min and incubated with antibodies against TMEM14A (1:1000, Sigma, Saint Louis, MO, USA), Bcl-2 (1:1000, Sigma, Saint Louis, MO, USA), Bax (1:1000, Sigma, Saint Louis, MO, USA), Cleaved-caspase-3 (1:1000, Sigma, Saint Louis, MO, USA) and GAPDH (1:1000, Sigma, Saint Louis, MO, USA) at 4°C overnight. GAPDH antibody was considered as the control. The membrane was then incubated with secondary antibodies (1:1000, Sigma, Saint Louis, MO, USA) at room temperature for 1 h and enhanced chemiluminescence (ECL) assay (Sigma, Saint Louis, MO, USA) was conducted to verify the protein bands.

Cell migration and invasion

For transwell migration assay, approximately 3×10^4 cells were seeded into the upper chamber without matrigel (Millipore, Bedford, MA, USA), and the medium containing 10% FBS was added into the lower chamber. After 24 h, the migratory cells were fixed with methanol and stained with crystal violet solution. Then, five fields were randomly selected to count the number of migrated cells by an inverted microscope (Olympus, Tokyo, Japan). After the upper chamber coated with matrigel, the invasion ability was detected with similar procedures.

Dual-luciferase reporter assay

StarBase (http://www.starBase.v3.0) and TargetScan (http://www.targetscan.org) were used to search for the assumed target of circFOXM1 and miR-132-3p. The wild-type (WT) or mutant (MUT) FOXM1 with or without potential miR-132-3p binding sites were constructed into the pmirGLO vectors (Promega, Madison, WI, USA). TMEM14A-WT and TMEM14A-MUT were obtained from Geneharma. Subsequently, the luciferase vectors were co-transfected into H1299 and A549 cells by Lipofectamine 3000 (Invitrogen, Carlsbad, CA, USA). After 48 h transfection, the luciferase activities were examined by a dual-luciferase reporter assay system (Promega, Madison, WI, USA).

Statistical analysis

All the data were calculated with SPSS 22.0, Student's *t*-test or one-way analysis of variance (ANOVA) was used to compare the groups' differences. The correlation among circFOXM1, miR-132-3p, and TMEM14A, was analyzed using Spearman correlation. $p < 0.05$ was regarded as significantly different.

Results

CircFOXM1 is up-regulated in NSCLC cells and tissue samples

The expression of circFOXM1 in 30 pairs of NSCLC tissues and adjacent normal tissues was detected by qRT-PCR, and the result indicated that circFOXM1 was significantly enhanced in NSCLC tissues ($p < 0.05$, Fig. 1(A)). Consistently, the expression level of circFOXM1 was significantly upregulated in NSCLC cell lines (SK-MES-1, H1299, and A549) compared with 16HBE cells ($p < 0.05$, Fig. 1(B)). The results suggested that circFOXM1 might be related to NSCLC progression.

Down-regulation of circFOXM1 inhibits NSCLC cell growth

To further explore the role of circFOXM1 in NSCLC, the siRNAs were used to repress circFOXM1 expression. QRT-PCT showed that circFOXM1 expression was down-regulated after the transfection with si-circFOXM1 in H1299 and A549 cells ($p < 0.05$, Fig. 2(A)). Moreover, MTT assay demonstrated that circFOXM1 knockdown inhibited the proliferation rates of H1299 and A549 cells ($p < 0.05$, Figs. 2(B)–2(C)). Our data showed that the proportion of apoptotic cells was significantly increased by circFOXM1 knockdown ($p < 0.05$, Fig. 2(D)). Besides, western blot results indicated that the expression of apoptosis-related proteins Bax and Cleaved-caspase-3 was increased, while the anti-apoptosis protein Bcl-2 was reduced in circFOXM1-silenced H1299 and A549 cells ($p < 0.05$, Figs. 2(E)–2(F)). The number of migrated and invaded H1299 and A549 cells was significantly decreased by circFOXM1 knockdown ($p < 0.05$, Figs. 2(G)–2(H)). Taken together, these results illustrated that circFOXM1 could regulate NSCLC cell growth, apoptosis, migration, and invasion.

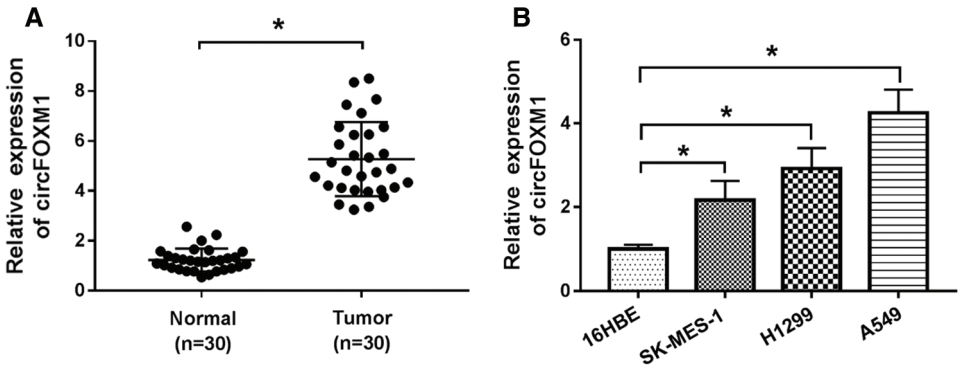

FIGURE 1. CircFOXM1 is up-regulated in NSCLC tissues and cells. (A) Relative expression of circFOXM1 in NSCLC tissue samples (n = 30) and their paired non-cancerous tissue samples (n = 30) was measured by qRT-PCR. (B) The expression of circFOXM1 in 16HBE, SK-MES-1, H1299, and A549 cells was detected by qRT-PCR. *$p < 0.05$.

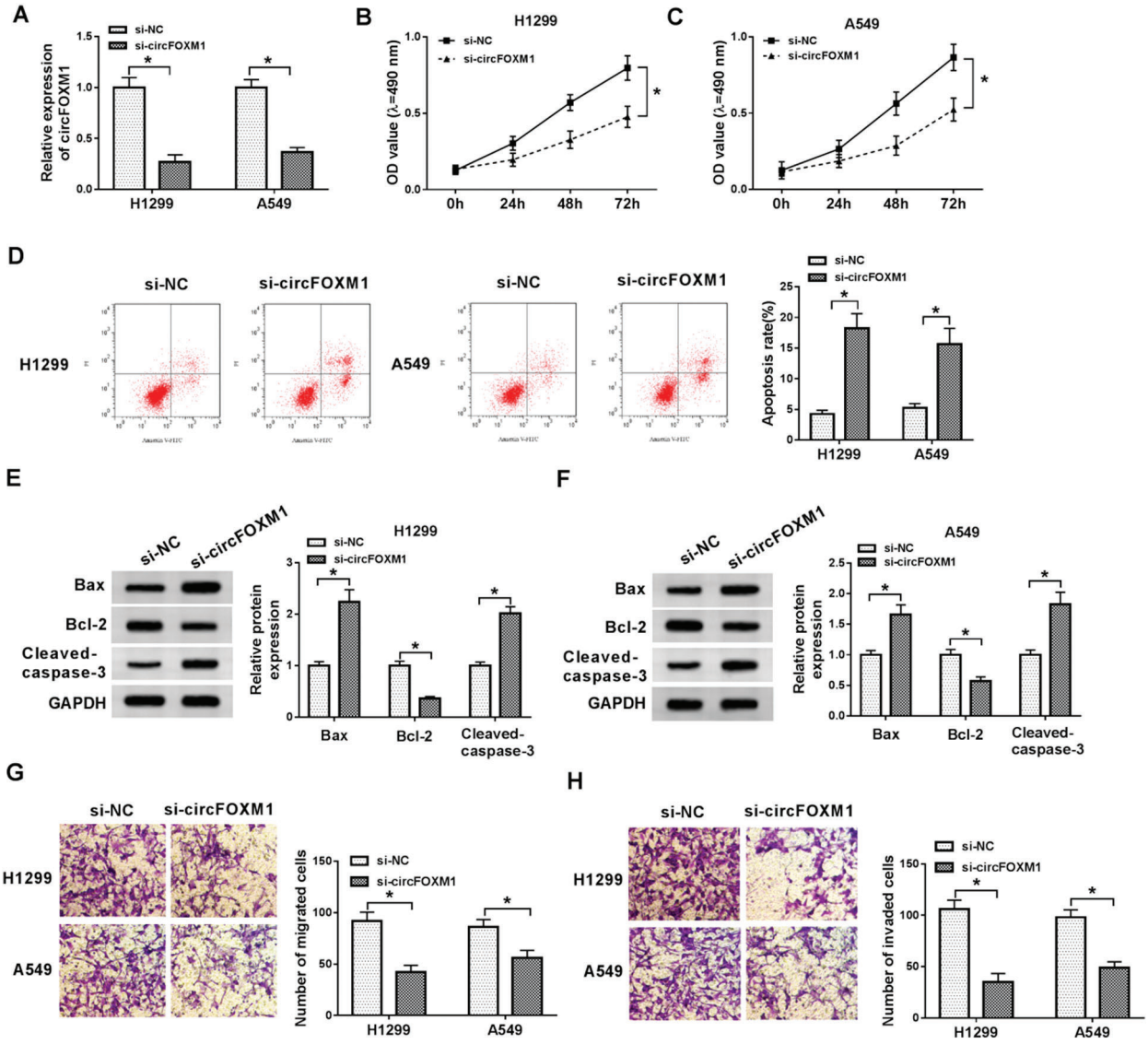

FIGURE 2. CircFOXM1 knockdown inhibits the proliferation, migration, and invasion and promoted cell apoptosis of NSCLC cells. (A) si-sircFOXM1 and si-NC were transfected into H1299 and A549 cells, and circFOXM1 expression was detected after transfection in H1299 and A549 cells by qRT-PCR. (B and C) MTT assay was employed to examine the cell viability of H1299 and A549 cells after transfection. (D) Flow cytometry assay was used to detect the apoptotic rate of H1299 and A549 cells after transfection. (E and F) The protein levels of Bax, Bcl-2, and Cleaved-caspase-3 were detected by western blot after transfection. (G and H) Transwell migration and invasion assays were used to detect cell migration and invasion capacities of H1299 and A549 cells after transfection. *$p < 0.05$.

CircFOXM1 acts as a molecular sponge for miR-132-3p in NSCLC

Starbase software was used to predict the potential binding sites between circFOXM1 and miR-132-3p (Fig. 3A). In addition, to examine whether miR-132-3p could bind to the predicted target sites of circFOXM1, the wild-type and mutant-type luciferase reporter vectors of circFOXM1 were constructed. As expected, co-transfection of miR-132-3p mimics and circFOXM1-WT luciferase vector, not circFOXM1-MUT, significantly repressed the luciferase activity of circFOXM1-WT ($p < 0.05$, Figs. 3(B)–3(C)). The expression of miR-132-3p in NSCLC specimens and normal tissues was examined by qRT-PCR, and the results showed that the expression level of miR-132-3p in NSCLC samples was lower than those in normal samples ($p < 0.05$, Fig. 3(D)). We further analyzed the relationship between circFOXM1 and miR-132-3p and found that circFOXM1 expression was negatively related to miR-132-3p expression in NSCLC tissue samples ($R = -0.551$, $p < 0.0001$, Fig. 3(E)). The expression of miR-132-3p was suppressed in NSCLC cells compared with the normal cells ($p < 0.05$, Fig. 3(F)). MiR-132-3p expression was up-regulated by si-circFOXM1 transfection, while circFOXM1 overexpression inhibited the expression of miR-132-3p ($p < 0.05$, Fig. 3(G)). These data indicated that circFOXM1 promoted NSCLC progression by sponging miR-132-3p.

The effects of circFOXM1 knockdown on tumorigenesis are partially reversed by miR-132-3p inhibitor

Rescue experiments were performed to detect whether circFOXM1 exerting carcinogenic functions by modulating miR-132-3p, and the results of qRT-PCR showed that miR-132-3p was promoted by si-circFOXM1, but the effect could be weakened by co-transfection with si-circFOXM1 and

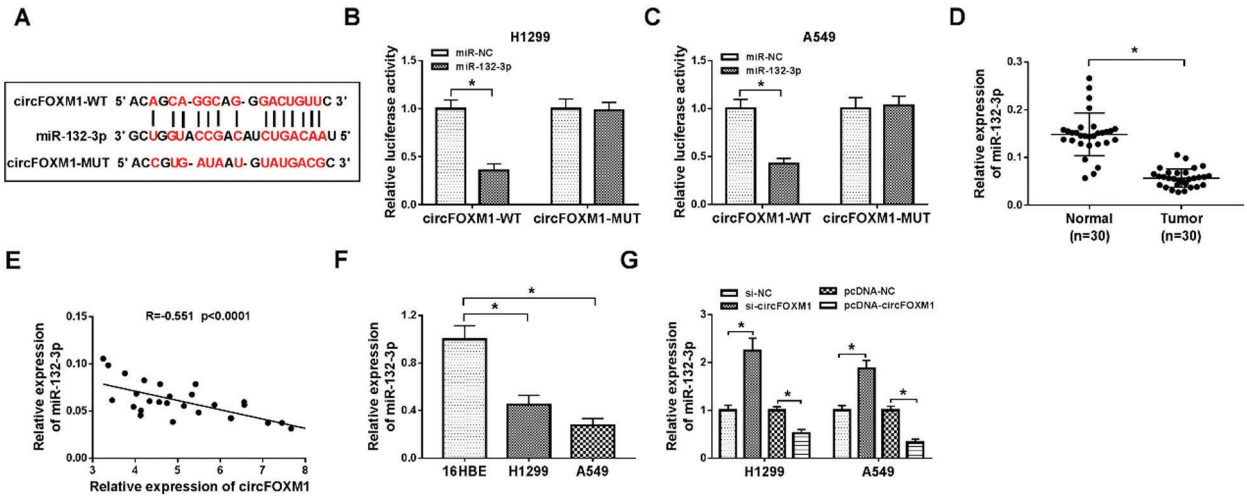

FIGURE 3. CircFOXM1 directly targets miR-132-3p.
(A) Putative miR-132-3p binding sites on circFOXM1 were predicted by biological software. (B and C) Dual-luciferase reporter assay was used to detect the correlation between circFOXM1 and miR-132-3p in H1299 and A549 cells. (D) The expression level of miR-132-3p in NSCLC tissues and normal tissues was detected by qRT-PCR. (E) Spearman's correlation analysis was used to detect the correlation between circFOXM1 expression and miR-132-3p expression. (F) miR-132-3p expression in 16HBE, H1299, and A549 cells was measured by qRT-PCR assay. (G) qRT-PCR was used to detect miR-132-3p expression in H1299 and A549 cells with transfection of circFOXM1 knockdown or circFOXM1 overexpression. *$p < 0.05$.

miR-132-3p inhibitor ($p < 0.05$, Fig. 4(A)). Silencing of miR-132-3p could abolish the inhibition effect of si-circFOXM1 on cell growth in H1299 and A549 cells ($p < 0.05$, Figs. 4(B)–4(C)). Moreover, miR-132-3p inhibitor impaired the increase of cell apoptosis rates triggered by circFOXM1 down-regulation ($p < 0.05$, Fig. 4(D)). Furthermore, circFOXM1 knockdown increased the protein levels of Bax and Cleaved-caspase-3 expression but decreased the expression of Bcl-2 expression. Nevertheless, these effects could be overturned by miR-132-3p silencing ($p < 0.05$, Figs. 4(E)–4(F)). Transwell assay indicated that cell migration and invasion were markedly decreased in H1299 and A549 cells with circFOXM1 down-regulation, while these effects were weakened by the miR-132-3p inhibitor ($p < 0.05$, Figs. 4(G)–4(H)). In addition, we also investigated the effect of anti-miR-132-3p on NSCLC progression and found that downregulation of miR-132-3p promoted cell proliferation, migration, and invasion in NSCLC cells (Supplemental Fig. S1). In brief, circFOXM1 contributed to NSCLC progression through regulating miR-132-3p.

TMEM14A is a target of miR-132-3p and regulated by circ-FOXM1

Bioinformatic analysis (www.starBase.v3.0) showed that TMEM14A might be regulated by miR-132-3p (Fig. 5(A)). Moreover, dual-luciferase reporter assay demonstrated that miR-132-3p inhibited the luciferase activity of TMEM14A-WT but not TMEM14A-MUT ($p < 0.05$, Figs. 5(B)–5(C)). TMEM14A was notably elevated in NSCLC tissues compared with normal tissues ($p < 0.05$, Figs. 5(D)–5(E)). Compared with 16HBE cells, the expression of TMEM14A was significantly up-regulated in H1299 and A549 cells ($p < 0.05$, Figs. 5(F)–5(G)). We further found that TMEM14A expression was negatively related to miR-132-3p expression ($R = -0.448$, $p < 0.0001$, Fig. 5(H)) and had a positive correlation with circFOXM1 level in NSCLC tissue samples ($R = 0.633$, $p < 0.0001$, Fig. 5(I)). TMEM14A expression level was down-regulated in H1299 and A549 cells transfected with miR-132-3p. Besides, overexpression of circFOXM1 reversed the decrease of TMEM14A expression induced by miR-132-3p ($p < 0.05$, Figs. 5(J)–5(L)). These findings elucidated that circFOXM1 could act as a sponge of miR-132-3p to enhance TMEM14A expression in NSCLC.

CircFOXM1 promotes NSCLC progression via up-regulating TMEM14A

qRT-PCR and western blot results indicated that the silencing of circ-FOXM1 reduced the level of TMEM14A, while TMEM14A overexpression partially restored the decrease ($p < 0.05$, Figs. 6(A)–6(C)). Next, MTT assay illustrated that abundant TMEM14A could partly reverse the tumor-suppressive functions in H1299 and A549 cells caused by si-circFOXM1 ($p < 0.05$, Figs. 6(D)–6(E)). Flow cytometry analysis implied that the apoptosis rates of H1299 and A549 cells transfected with si-circFOXM1 were dramatically increased compared with the si-NC group, while the increase was abrogated by pcDNA-TMEM14A ($p < 0.05$, Fig. 6(F)). To further explore whether the decrease of apoptosis was caused by activation of the intracellular apoptotic pathway, western blot analysis was used to quantify the protein expression of Bax, Bcl-2, and Cleaved caspase-3. Our results indicated that the protein levels of Bax and Cleaved caspase-3 were significantly increased, and the protein level of Bax was apparently decreased in the si-circFOXM1 group, while overexpression of TMEM14A inverted these effects ($p < 0.05$, Figs. 6(G)–6(H)). Similarly, circFOXM1 knockdown could significantly impede the migration and invasion abilities of H1299 and A549 cells, but the effects could be abolished by TMEM14A overexpression ($p < 0.05$, Figs. 6(I)–6(J)). Overall, these results demonstrated that circFOXM1 mediated the

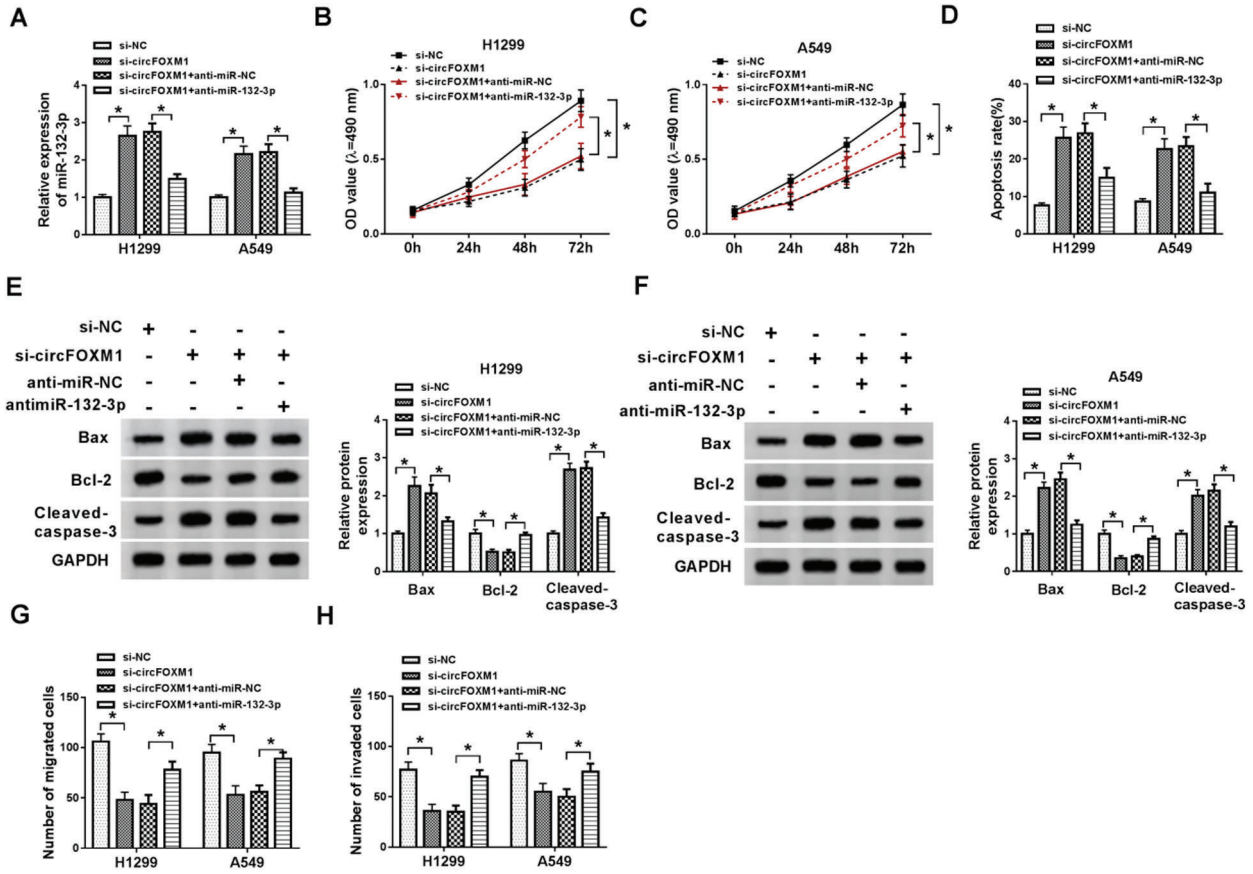

FIGURE 4. MiR-132-3p reverses the effects of circFOXM1 knockdown on H1299 and A549 cells.
(A) The expression of miR-132-3p was analyzed by qRT-PCR in H1299 and A549 cells co-transfected with si-NC or si-circFOXM1 and miR-NC inhibitor or miR-132-3p inhibitor. (B and C) MTT assay was performed to detect the growth ability of H1299 and A549 cells co-transfected with si-NC or si-circFOXM1 and miR-NC inhibitor or miR-132-3p inhibitor. (D) Flow cytometry assay was applied to measure the apoptosis of H1299 and A549 cells co-transfected with si-NC or si-circFOXM1 and miR-NC inhibitor or miR-132-3p inhibitor. (E and F) The protein levels of apoptosis-related genes (Bax, Bcl-2, and Cleaved-caspase-3) in H1299 and A549 cells co-transfected with si-NC or si-circFOXM1 and miR-NC inhibitor or miR-132-3p inhibitor were determined by western blot. (G and H) Transwell assay was performed to assess cell migration and invasion in H1299 and A549 cells co-transfected with si-NC or si-circFOXM1 and miR-NC inhibitor or miR-132-3p inhibitor. *$p < 0.05$.

proliferation, apoptosis, migration, and invasion of NSCLC cells via regulating TMEM14A.

Discussion

We found that circFOXM1 was elevated in NSCLC tissues. Knockdown of circFOXM1 greatly suppressed the abilities of proliferation, migration, and invasion, and obviously promoted the apoptosis of the H1299 and A549 cells, exhibiting the anti-tumor effect. Moreover, low expression of miR-132-3p was found in NSCLC tissues and negatively regulated by circFOXM1. Besides, the interaction between circFOXM1 and miR-132-3p was predicted by bioinformatics analysis and confirmed by dual-luciferase reporter assay, suggesting that there was a target relationship between circFOXM1 and miR-132-3p. It could be inferred that circFOXM1 played a carcinogenic role in H1299 and A549 cells by targeting miR-132-3p.

Recent pieces of research found that cyclic RNA was a subset of the ncRNA family and played a significant role in the progression of multiple cancers (Li *et al.*, 2015a). For example, Rong *et al.* (2019) showed that has-circ-0007534 downregulation inhibited cell growth of cervical cancer via regulating the miR-498/BMI-1 axis. CircMYLK was augmented in hepatocellular carcinoma tissues and cells and promoted cell proliferation and invasion by inactivating the constraint of miR-362-3p to regulate Rab23 expression (Li *et al.*, 2019b). Hsa_circRNA_102958 promoted tumor metastasis *in vivo* by inducing the proliferation and migration of gastric cancer cells through the activation of the miR-585/CDC25B axis (Li *et al.*, 2019c). Liu *et al.* (2019b) revealed that circFOXM1 was overexpressed and contributed to carcinogenic progression as a competitive endogenous RNA to target PPDPF and MACC1 through sponging miR-1304-5p in NSCLC. Similar results were also presented in our research, exceptionally expression of circFOXM1 was associated with the progression of NSCLC. The knockdown of circFOXM1 resulted in a drastic decrease in NSCLC cell viability by regulating a few cellular programs. The alteration of apoptosis, migration, and invasion was related to the occurrence and development of tumors, while the deregulation of the apoptotic cell death mechanism was a symbol of cancer (Pistritto *et al.*, 2016). Therefore, Bax, Bcl-2, and Cleaved caspase-3 were the primarily secreted proteins that were necessary for the supervision of apoptosis (Charununtakorn *et al.*, 2016).

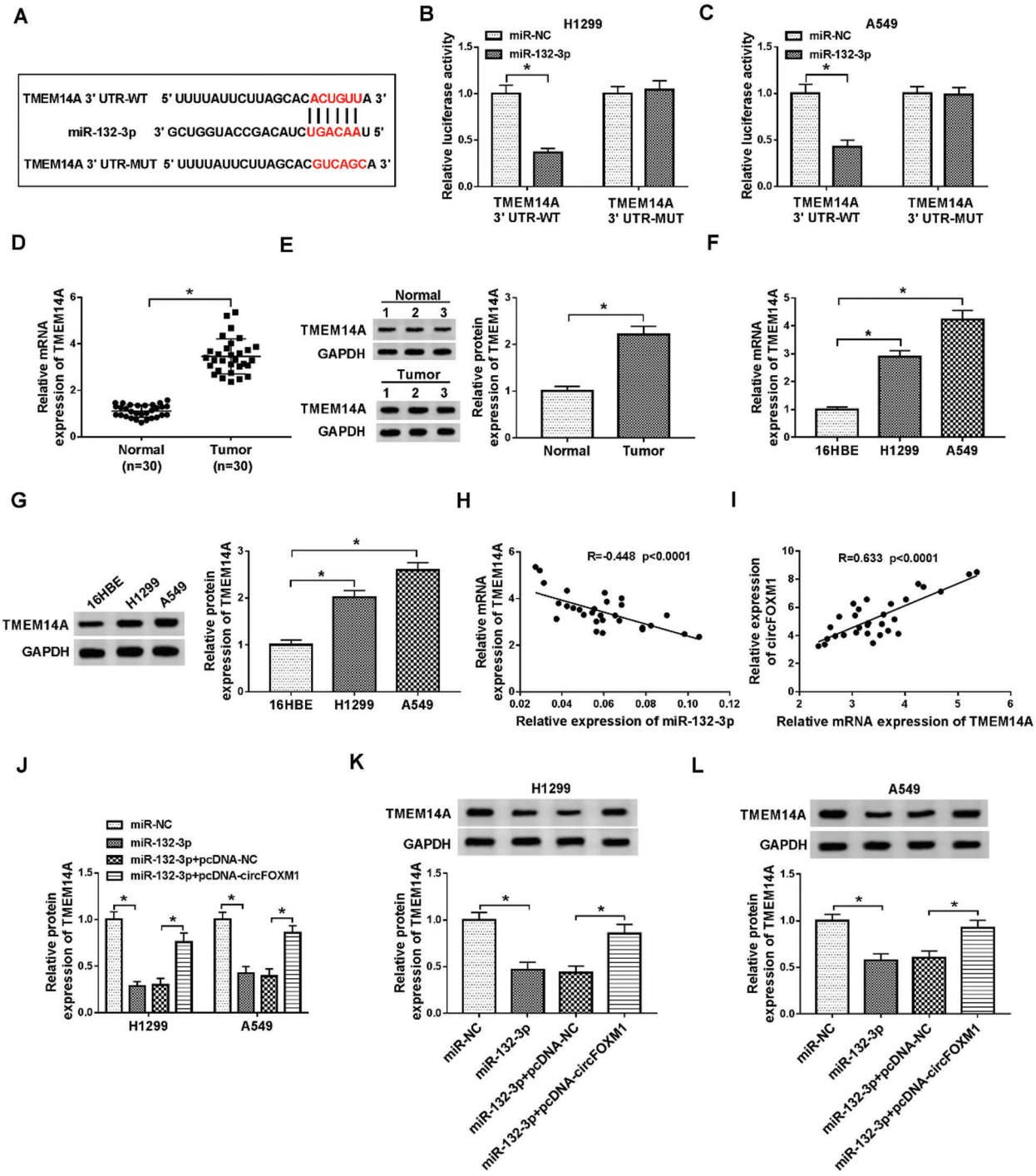

FIGURE 5. TMEM14A is a target gene of miR-132-3p.
(A) Binding sites between miR-132-3p and TMEM14A were predicted using the bioinformatics database. (B and C) TMEM14A-WT vectors or TMEM14A-MUT vectors and miR-132-3p mimics or miR-NC were transfected into H1299 and A549 cells, and the luciferase activity was measured. (D and E) The mRNA and protein levels of TMEM14A in NSCLC tissues and normal tissues were determined by qRT-PCR and western blot. (F and G) The mRNA and protein levels of TMEM14A in 16HBE, H1299, and A549 cells were determined by qRT-PCR and western blot. (H and I) The correlation between the miR-132-3p level and TMEM14A expression (or circFOXM1 expression) was measured by Spearman's correlation. (J, K, and L) The mRNA and protein levels of TMEM14A in H1299 and A549 cells co-transfected with miR-NC or miR-132-3p and pcDNA-NC or pcDNA-circFOXM1 were determined by qRT-PCR and western blot. *$p < 0.05$.

It was well known that abnormally expressed miRNA has a close correlation with the occurrence of tumors (Kurozumi *et al.*, 2017). For example, miR-145 expression was markedly inhibited in gastric cancer cells, which could restrain the proliferation ability of gastric cancer cells and enhance apoptosis (Wang *et al.*, 2019b). Ma *et al.* (2019) pointed out that miR-100, which was situated in human chromosome 11q24.1 location, was reduced in NSCLC, and miR-100 overexpression was closely related to the good prognosis of NSCLC patients. Moreover, miR-132-3p can negatively regulate the expression of tumor-related target genes. Interestingly, similar results were found in our research, as a

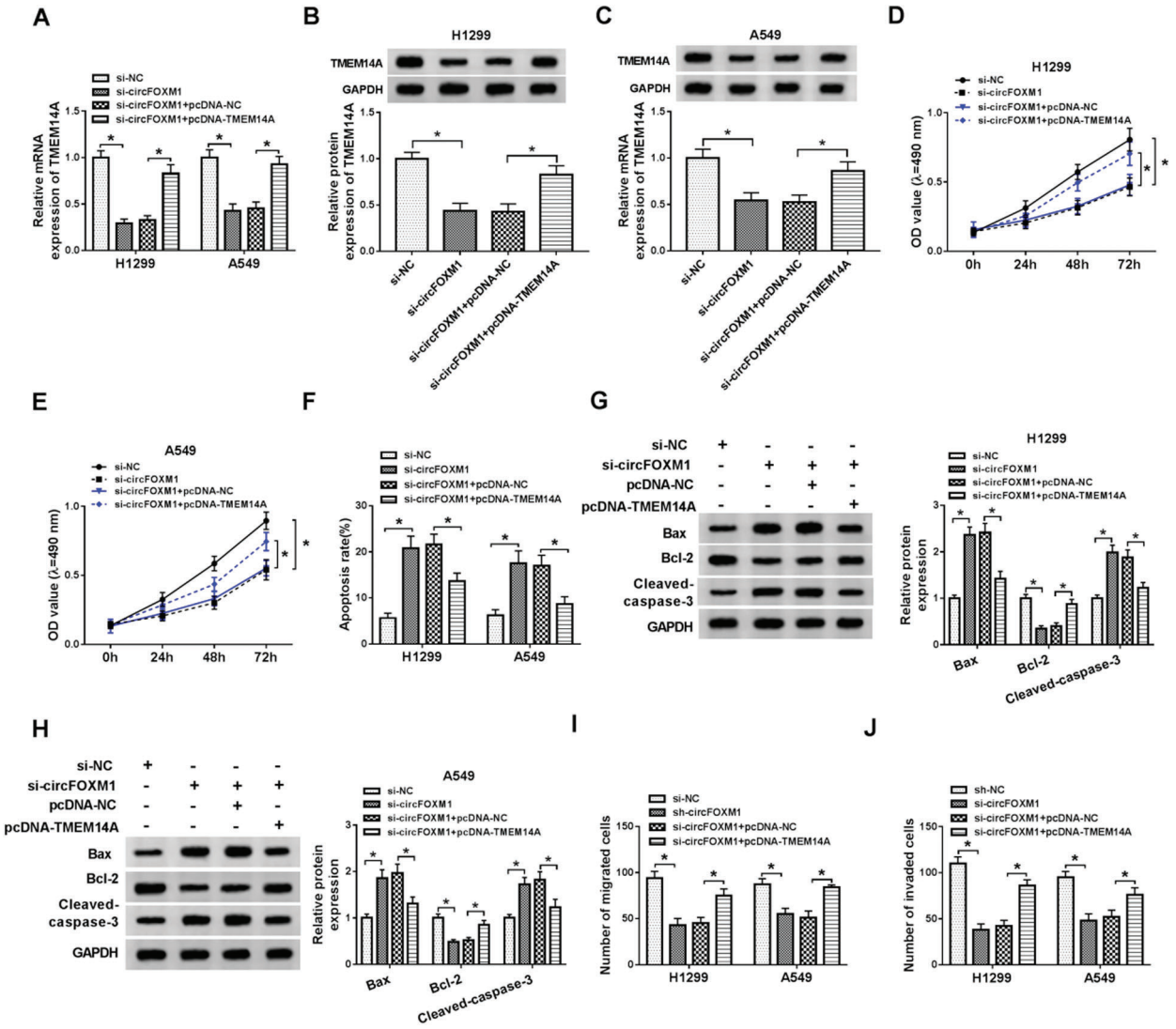

FIGURE 6. TMEM14A overexpression overturns the effects of circFOXM1 knockdown on NSCLC progression.
(A, B and C) The mRNA and protein levels of TMEM14A were detected by qRT-PCR and western blot in H1299 and A549 cells co-transfected with si-circFOXM1 or si-circFOXM1 + pcDNA-TMEM14A. (D and E) Cell viability of H1299 and A549 cells co-transfected with si-circFOXM1 or si-circFOXM1 + pcDNA-TMEM14A was measured at the indicated time points by MTT assay. (F) Flow cytometry was used to examine the apoptosis of H1299 and A549 cells co-transfected with si-circFOXM1 or si-circFOXM1 + pcDNA-TMEM14A cells. (G and H) Protein expression levels of Bax, Bcl-2, and Cleaved-caspase-3 were measured at 48 h in H1299 and A549 cells co-transfected with si-circFOXM1 or si-circFOXM1 + pcDNA-TMEM14A cells. (I and J) Transwell assay was used to determine the migration and invasion of H1299 and A549 cells co-transfected with si-circFOXM1 or si-circFOXM1 + pcDNA-TMEM14A. *$p < 0.05$.

downstream target of circFOXM1, miR-132-3p had the opposite effects on cell proliferation, apoptosis, migration, and invasion of H1299 and A549 cells.

TMEM14A is a mitochondrial-related membrane protein that contains three transmembrane domains (Zhang *et al.*, 2016). TMEM14A was found to be a novel Bax and caspase-3 inhibitor, which might be an inhibitor of cell death. Previous researches showed that TMEM14A prevented N-(4-hydroxyphenyl) retinamide induced apoptosis by stabilizing mitochondrial apoptosis pathway (Woo *et al.*, 2011). Moreover, a recent study confirmed that TMEM14A played a fateful role in the emergence and metastasis of tumors. TMEM14A was overexpressed in NSCLC and triggered the invasion and migration of NSCLC cells (An *et al.*, 2019). Zhang *et al.* (2016) demonstrated that inactivation of TMEM14A impaired cell progression in ovarian cancer. Moreover, TMEM14A held a momentous position in ovarian cancer (Zhang *et al.*, 2016). All the conclusions verified the tumorigenicity of TMEM14A in a variety of tumors. We found that suppression of circFOXM1 prevented TMEM14A expression level by sponging miR-132-3p in NSCLC cells. Thus, we could speculate that circFOXM1 played a carcinogenic role by up-regulating TMEM14A expression and competing for miR-132-3p expression, leading to the enrichment of TMEM14A and accelerated the development of NSCLC.

Undoubtedly, circFOXM1, miR-132-3p, and TMEM14A are pivotal for cancer regulation. Referring to the investigation, we could suppose that circFOXM1 had a carcinogenic effect through sponging miR-132-3p and elevating TMEM14A in NSCLC progression. However, the lack of abundant clinic samples and survival analysis were

the main limitations of the research. Furthermore, the functions of circFOXM1 should be verified *in vivo* experiments.

Conclusions

In brief, we found that circFOXM1 might exhibit a favorable role in cell survival by regulating TMEM14A through sponging miR-132-3p in NSCLC cells.

Availability of Data and Materials: The data used and/or analyzed during the current study are available from the corresponding author on reasonable request.

Author Contribution: Study conception and design: Weigao Zhong; data collection: Aiqin Chen and Xiaohong Tang; analysis and interpretation of results: Aiqin Chen and Yi Liu; draft manuscript preparation: Weigao Zhong. All authors reviewed the results and approved the final version of the manuscript.

Ethics Approval: Written informed consents were obtained from all participants and this study was permitted by the Ethics Committee of Sichuan Mianyang 404 Hospital (IRB No. 2016MY662, Approval Date: 2016.06.18).

Funding Statement: The author(s) received no specific funding for this study.

Conflicts of Interest: The authors declare that they have no conflicts of interest to report regarding the present study.

References

An J, Shi H, Zhang N, Song S (2019). Elevation of circular RNA circ_0003645 forecasts unfavorable prognosis and facilitates cell progression via miR-1179/TMEM14A pathway in non-small cell lung cancer. *Biochemical and Biophysical Research Communications* **511**: 921–925. DOI 10.1016/j.bbrc.2019.03.011.

Charununtakorn ST, Shinlapawittayatorn K, Chattipakorn SC, Chattipakorn N (2016). Potential roles of humanin on apoptosis in the heart. *Cardiovascular Therapies* **34**: 107–114. DOI 10.1111/1755-5922.12168.

Chen JY, Hour TC, Yang SF, Chien CY, Chen HR, Tsai KL, Ko JY, Wang LF (2015). Autophagy is deficient in nasal polyps: implications for the pathogenesis of the disease. *International Forum of Allergy & Rhinology* **5**: 119–123. DOI 10.1002/alr.21456.

Chen T, Shao S, Li W, Liu Y (2019). The circular RNA hsa-circ-0072309 plays anti-tumour roles by sponging miR-100 through the deactivation of PI3K/AKT and mTOR pathways in the renal carcinoma cell lines. *Artificial Cells, Nanomedicine, and Biotechnology* **47**: 3638–3648. DOI 10.1080/21691401.2019.1657873.

Didkowska J, Wojciechowska U, Manczuk M, Lobaszewski J (2016). Lung cancer epidemiology: contemporary and future challenges worldwide. *Annals of Translational Medicine* **4**: 150. DOI 10.21037/atm.2016.03.11.

Jeck WR, Sorrentino JA, Wang K, Slevin MK, Burd CE, Liu J, Marzluff WF, Sharpless NE (2013). Circular RNAs are abundant, conserved, and associated with ALU repeats. *RNA* **19**: 141–157. DOI 10.1261/rna.035667.112.

Jemal A, Bray F, Center MM, Ferlay J, Ward E, Forman D (2011). Global cancer statistics. *CA: A Cancer Journal for Clinicians* **61**: 69–90.

Kristensen LS, Hansen TB, Veno MT, Kjems J (2018). Circular RNAs in cancer: opportunities and challenges in the field. *Oncogene* **37**: 555–565. DOI 10.1038/onc.2017.361.

Kurozumi A, Goto Y, Okato A, Ichikawa T, Seki N (2017). Aberrantly expressed microRNAs in bladder cancer and renal cell carcinoma. *Journal of Human Genetics* **62**: 49–56. DOI 10.1038/jhg.2016.84.

Li P, Chen S, Chen H, Mo X, Li T, Shao Y, Xiao B, Guo J (2015a). Using circular RNA as a novel type of biomarker in the screening of gastric cancer. *Clinica Chimica Acta* **444**: 132–136. DOI 10.1016/j.cca.2015.02.018.

Li X, Chen SH, Zeng JW (2019a). MiR-421 is overexpressed and promotes cell proliferation in non-small cell lung cancer. *Medical Principles and Practice* **29**: 80–89. DOI 10.1159/000503020.

Li Z, Hu Y, Zeng Q, Wang H, Yan J, Li H, Yu Z (2019b). Circular RNA MYLK promotes hepatocellular carcinoma progression by increasing Rab23 expression by sponging miR-362-3p. *Cancer Cell International* **19**: 211. DOI 10.1186/s12935-019-0926-7.

Li Y, Huang S (2017). Response to Comment on Response to "Circular RNA Profile Identifies circPVT1 as a Proliferative Factor and Prognostic Marker in Gastric Cancer," Cancer Lett. 2017 Mar 1; 388(2017): 208-219. *Cancer Letters* **411**: 64. DOI 10.1016/j.canlet.2016.12.006.

Li R, Wu B, Xia J, Ye L, Yang X (2019c). Circular RNA hsa_circRNA_102958 promotes tumorigenesis of colorectal cancer via miR-585/CDC25B axis. *Cancer Management Research* **11**: 6887–6893. DOI 10.2147/CMAR.S212180.

Li Y, Zu L, Wang Y, Wang M, Chen P, Zhou Q (2015b). miR-132 inhibits lung cancer cell migration and invasion by targeting SOX4. *Journal of Thoracic Disease* **7**: 1563–1569.

Liu KS, Pan F, Mao XD, Liu C, Chen YJ (2019a). Biological functions of circular RNAs and their roles in occurrence of reproduction and gynecological diseases. *American Journal of Translational Research* **11**: 1–15.

Liu G, Shi H, Deng L, Zheng H, Kong W, Wen X, Bi H (2019b). Circular RNA circ-FOXM1 facilitates cell progression as ceRNA to target PPDPF and MACC1 by sponging miR-1304-5p in non-small cell lung cancer. *Biochemical and Biophysical Research Communications* **513**: 207–212. DOI 10.1016/j.bbrc.2019.03.213.

Ma X, Zhou J, Mo H, Ying Y (2019). Association of miR-100 expression with clinicopathological features and prognosis of patients with lung cancer. *Oncology Letters* **18**: 1318–1322.

Macfarlane LA, Murphy PR (2010). MicroRNA: biogenesis, function and role in cancer. *Current Genomics* **11**: 537–561. DOI 10.2174/138920210793175895.

Memczak S, Jens M, Elefsinioti A, Torti F, Krueger J, Rybak A, Maier L, Mackowiak SD, Gregersen LH, Munschauer M, Loewer A, Ziebold U, Landthaler M, Kocks C, le Noble F, Rajewsky N (2013). Circular RNAs are a large class of animal RNAs with regulatory potency. *Nature* **495**: 333–338. DOI 10.1038/nature11928.

Pistritto G, Trisciuoglio D, Ceci C, Garufi A, D'Orazi G (2016). Apoptosis as anticancer mechanism: function and dysfunction of its modulators and targeted therapeutic strategies. *Aging* **8**: 603–619.

Rong X, Gao W, Yang X, Guo J (2019). Downregulation of hsa_circ_0007534 restricts the proliferation and invasion of cervical cancer through regulating miR-498/BMI-1 signaling. *Life Sciences* **235**: 116785. DOI 10.1016/j.lfs.2019.116785.

Taborda MI, Ramirez S, Bernal G (2017). Circular RNAs in colorectal cancer: possible roles in regulation of cancer cells. *World Journal of Gastrointestinal Oncology* **9**: 62–69. DOI 10.4251/wjgo.v9.i2.62.

Wang H, Sha L, Huang L, Yang S, Zhou Q, Luo X, Shi B (2019a). LINC00261 functions as a competing endogenous RNA to regulate BCL2L11 expression by sponging miR-132-3p in endometriosis. *American Journal of Translational Research* **11**: 2269–2279.

Wang J, Sun Z, Yan S, Gao F (2019b). Effect of miR145 on gastric cancer cells. *Molecular Medicine Reports* **19**: 3403–3410.

Wang XQ, Zhang Y, Hou W, Wang YT, Zheng JB, Li J, Lin LZ, Jiang YL, Wang SY, Xie Y, Zhang HL, Shu QJ, Li P, Wang W, You JL, Li G, Liu J, Fan HT, Zhang MY, Lin HS (2019c). Association between Chinese medicine therapy and survival outcomes in postoperative patients with NSCLC: a multicenter, prospective, cohort study. *Chinese Journal of Integrative Medicine* **25**: 812–819. DOI 10.1007/s11655-019-3168-6.

Woo IS, Jin H, Kang ES, Kim HJ, Lee JH, Chang KC, Park JY, Choi WS, Seo HG (2011). TMEM14A inhibits N-(4-hydroxyphenyl)retinamide-induced apoptosis through the stabilization of mitochondrial membrane potential. *Cancer Letters* **309**: 190–198. DOI 10.1016/j.canlet.2011.05.031.

Wu L, Zhang M, Qi L, Zu X, Li Y, Liu L, Chen M, Li Y, He W, Hu X, Mo M, Ou Z, Wang L (2019). ERα-mediated alterations in circ_0023642 and miR-490-5p signaling suppress bladder cancer invasion. *Cell Death & Disease* **10**: 635. DOI 10.1038/s41419-019-1827-3.

You J, Li Y, Fang N, Liu B, Zu L, Chang R, Li X, Zhou Q (2014). MiR-132 suppresses the migration and invasion of lung cancer cells via targeting the EMT regulator ZEB2. *PLoS One* **9**: e91827. DOI 10.1371/journal.pone.0091827.

Zhang Q, Chen X, Zhang X, Zhan J, Chen J (2016). Knockdown of TMEM14A expression by RNAi inhibits the proliferation and invasion of human ovarian cancer cells. *Bioscience Reports* **36**: e00298. DOI 10.1042/BSR20150258.

Zhang D, Yang XJ, Luo QD, Fu DL, Li ZL, Zhang P, Chong T (2019). Down-regulation of circular RNA_000926 attenuates renal cell carcinoma progression through microRNA-411-dependent CDH2 inhibition. *American Journal of Pathology* **189**: 2469–2486. DOI 10.1016/j.ajpath.2019.06.016.

Zhou C, Zhang Y, Dai J, Zhou M, Liu M, Wang Y, Chen XZ, Tang J (2016). Pygo2 functions as a prognostic factor for glioma due to its up-regulation of H3K4me3 and promotion of MLL1/MLL2 complex recruitment. *Scientific Reports* **6**: 22066. DOI 10.1038/srep22066.

Appendix

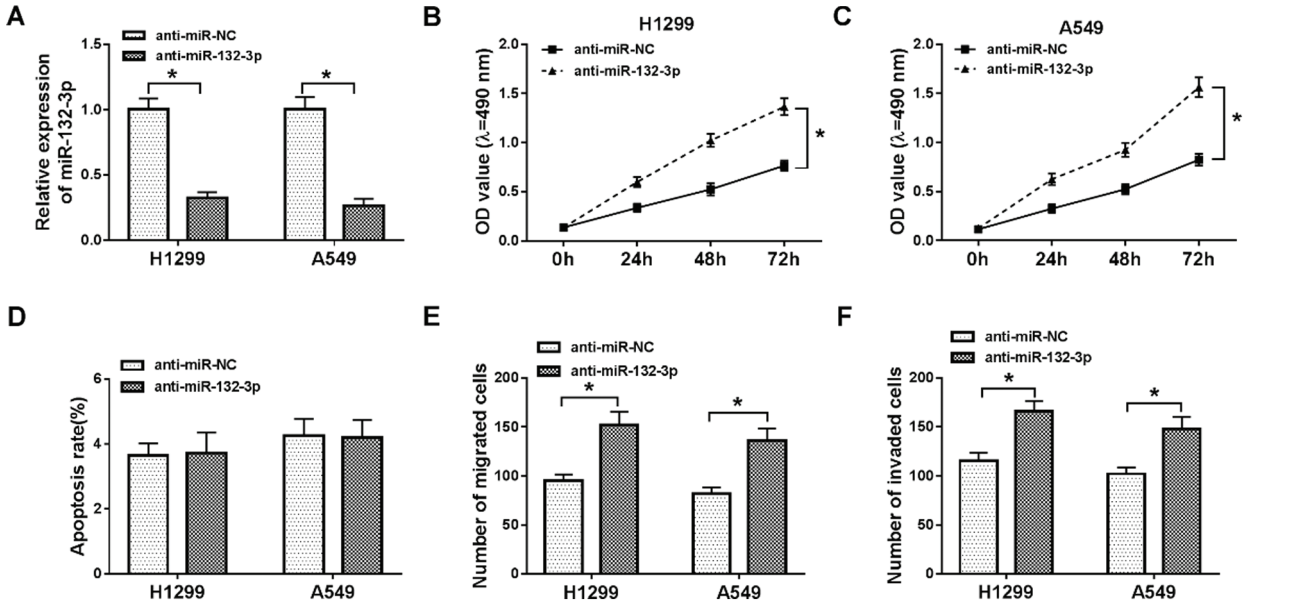

SUPPLEMENTAL FIGURE S1. MiR-132-3p depletion boosts the proliferation, migration, and invasion of NSCLC cells.
(A) The expression level of miR-132-3p in NSCLC cells transfected with anti-miR-NC or anti-miR-132-3p was measured by qRT-PCR. (B and C) MTT assay was used to detect cell proliferation. (D) Flow cytometry was used to detect cell apoptosis. (E and F) Transwell migration and invasion assays were utilized to measure the capacities of cell migration and invasion. $^*P < 0.05$.